Proc. NIPR Symp. Upper Atmos. Phys., 1, 56–64, 1988

AURORAL X-RAY IMAGE FORMINGS USING THREE DIRECTIONAL NaI (Tl) TELESCOPES AT BALLOON ALTITUDE

Masahiro KODAMA[1], Shigeo OHTA[2], Takamasa YAMAGAMI[2], Michiyoshi NAMIKI[2], Jun NISHIMURA[2], Yo HIRASIMA[3], Hiroyuki MURAKAMI[3], Kiyoaki OKUDAIRA[3], Hiromu SUZUKI[3], Hiroshi MIYAOKA[4], Natsuo SATO[4] and Ryoichi FUJII[4]

[1]*Department of Physics, Yamanashi Medical College, Tamaho, Nakakoma, Yamanashi 409–38*
[2]*The Institute of Space and Astronautical Science, 6–1, Komaba 4-chome, Meguro-ku, Tokyo 153*
[3]*Department of Physics, Rikkyo University, 34–1, Nishi-Ikebukuro 3-chome, Toshima-ku, Tokyo 171*
[4]*National Institute of Polar Research, 9–10, Kaga 1-chome, Itabashi-ku, Tokyo 173*

Abstract: This report presents the spatial distributions of auroral X-rays obtained by the balloon flight named AZCO-C1, which was launched from Norway in July 1985. A time sequence of auroral X-ray images were derived by using a set of three NaI (Tl) scintillation counters for each of the three different energy channels: 22–35, 35–55 and 55–88 keV. The precipitation region of energetic particles and its modulations with time were well demonstrated, though the X-ray enhancements were only three times the background flux.

1. Introduction

Recently, numerous experimental investigations of auroral X-ray images have been performed with respect to the structured precipitation of energetic electrons in high latitudes, by means of balloon, rocket and satellite (*e.g.*, IMHOF *et al.*, 1985; GOLDBERG *et al.*, 1982; KREMSER *et al.*, 1982). Though the satellite observation provides certainly a lot of data covering the both hemispheres, a complete separation of the spatial information from the temporal one is rather difficult inherently. The observation time allowable for the rocket experiment is usually restricted to 10 min or so. Since the Bremsstrahlung X-rays from energetic electrons impinging into the atmosphere are detectable even at a deep atmosphere of balloon altitude, simple and economical types of X-ray imagers still play an important role in this field of research. For example, one imager is a scanning telescope consisting of inclined directional X-ray detectors, single or plural (PARKS 1967; YAMAGAMI *et al.*, 1978). Another one is a device of one-shot camera, with a single-pinhole (MAUK *et al.*, 1981; HIRASIMA *et al.*, 1987), or with multi-pinholes (HIRASIMA *et al.*, 1983; CALVERT *et al.*, 1985).

The balloon observation reported here was carried out in July 1985, as one of the AZCO (Auroral Zone Conjugate Observation) campaign under the international cooperation among three countries of Denmark, Norway and Japan. A set of three directional NaI (Tl) scintillation counters were used to measure the energy-dependent structures of auroral X-ray images by sky scanning.

The main purpose of this campaign was to investigate the geomagnetic conjugacy

in particle precipitation and wave propagation between the northern and the southern hemispheres. To accomplish this aim successfully, the expected cruise of the balloon was taken so as to pass over the vicinity of Iceland, which forms the best conjugate pair with Syowa Station, Antarctica. Significant enhancements of X-ray fluxes were observed three times during the ceiling altitude flight of about 45 h after launch, but in two of them the acquired data were unreliable due to telemetry interferences. In this report the X-ray data obtained from the remaining one are analyzed mainly with respect to spatial distributions and their time modulations.

2. Instrumentation and Flight Description

The X-ray instrument used consists of three sets of NaI (Tl) scintillation detectors, 1.5-inch in diameter and 3-mm in thickness, arranged obliquely by 17.5° from the zenith, pointing to three different azimuths 120° apart one another. Each detector has a full field of view of 35° collimated by using a sandwich plate composed of 1-mm thick Pb and 2-mm thick Sn. Thus the whole field of view of this instrument covers a circular area of about 100 km in diameter, as seen in Fig. 1, assuming the height of X-ray producing layer as 100 km.

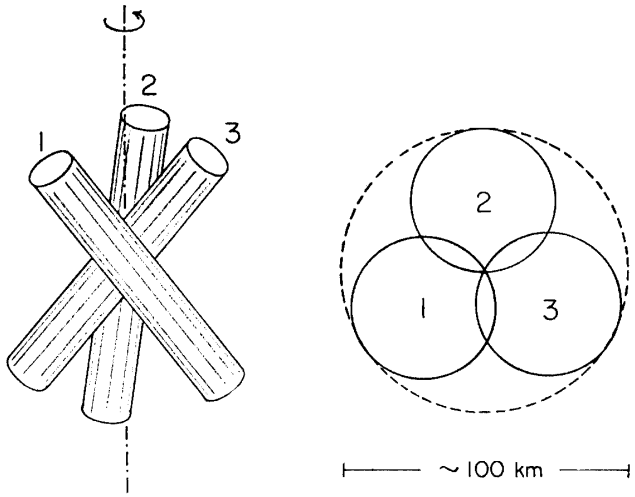

Fig. 1. Orientation and identification of the balloon-borne X-ray detector.

The following four different energy channels were selected for the measurement; 22–35 keV, 35–55 keV, 55–88 keV and >88 keV. The payload gondola containing the X-ray instrument and the house keeping equipments was designed to rotate around its vertical axis with a constant period of 45 s. The sampling rate of the data consisting of 22 channels was taken as 1/16 s, so as to be capable of discriminating rapid flux fluctuations such as microburst phenomena. All of the data were telemetered by means of the PCM system.

The balloon AZCO-C1 was launched from Abelbar, Norway, at 2107 UT on July 2, 1985, and then flew westward in a latitudinal range from 54°N to 67°N. After 45-h level flight at a ceiling altitude of 32 km, the gondola was dropped down in the

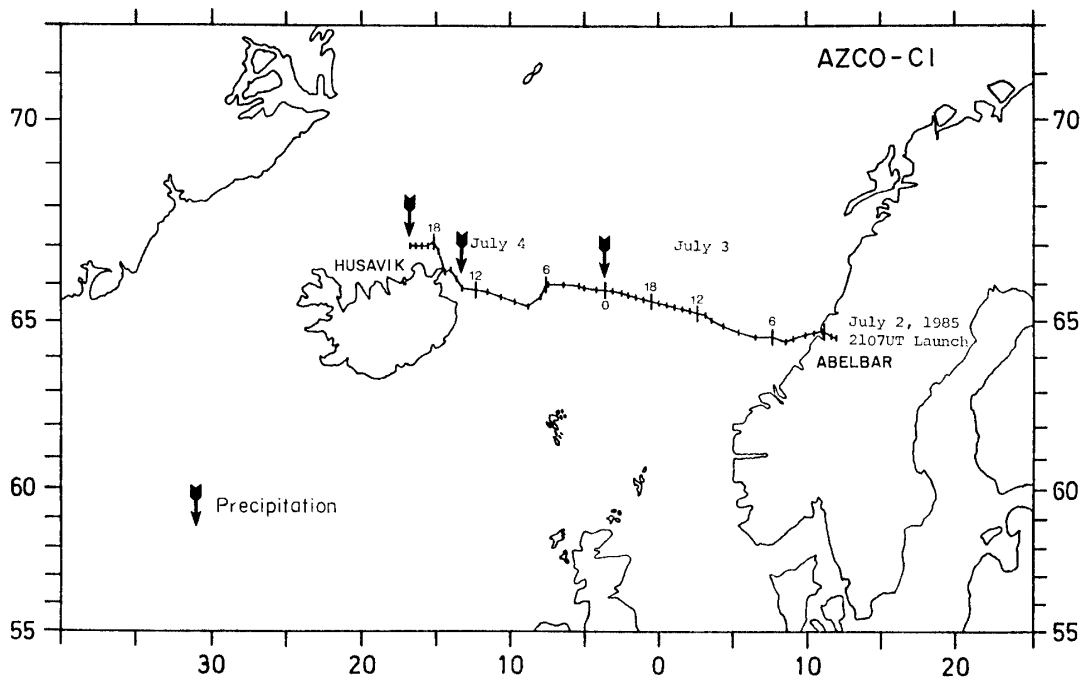

Fig. 2. Trajectory of the balloon flight AZCO-C1.

vicinity of Iceland at 2211 UT on July 4. Figure 2 shows the entire flight cruise, in which three arrows indicate the locations where significant particle precipitation events were observed.

Unfortunately, reliable data were missed from two of the three precipitation events because of telemetry troubles. The first missing was found around at 0 UT on July 4, when the balloon was located farthest apart from each of the two radio receiving stations, Abelbar in Norway and Husavik in Iceland. The other one was a few

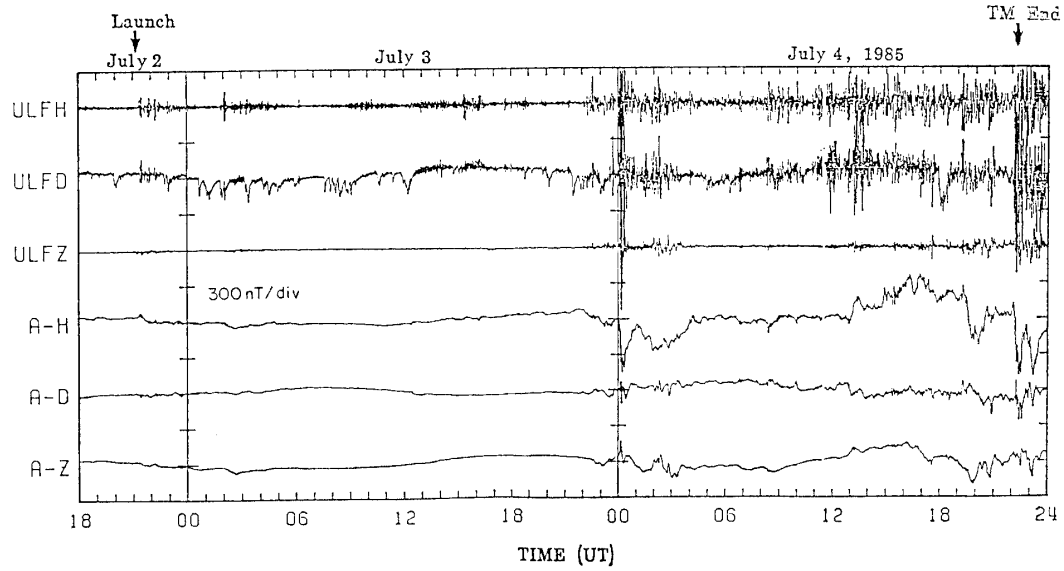

Fig. 3. Records of the ordinary and pulsative geomagnetic field observed at Husafell, Iceland, during the flight of AZCO-C1.

hours just before the rope cut, when the balloon was located in the shade of mountains near Husavik. Radar trackings of the balloon positions were performed successfully by the ARGOS system.

General aspect of the geomagnetic activity during the flight is shown in Fig. 3, with magnetograms from ordinary and induction magnetometers. It is evident from the figure that the activity was quite calm on July 3, but there occurred moderate disturbances in the latter half of the flight.

3. Observation Results

The second precipitation event occurred during 13–15 UT on July 4 contains two small X-ray enhancements (hereafter denoted by event-1 and event-2, respectively). Figures 4a and 4b show time profiles of 1-s counts recorded by the three different counters, except for the highest energy channel of >88 keV. A sinusoidal wave given at the bottom of the figures is the record of the geomagnetic aspectometer (GA), showing a stable rotation of the payload gondola with a period of 45 s.

It is evident from the gross feature of the time profiles shown in Fig. 4 that the amplitude of enhancement decreases with increasing energy of X-rays in event-1, but that the enhancement from the mid-energy channel of 35–55 keV in event-2 is most predominant. The maximum counts of the enhancements are not beyond five times the background counts for all channels. Thus the following statistical method of analysis was applied to find out every modulation occurred during the time interval of interest.

Since any one azimuthal direction is scanned three times by each of the three counters every 15 s during one rotation period, counting rates from each can be added within the identical field of view, if a flux distribution stays stable during one rotation. Of course, it is impossible on this way to discriminate any non-uniformity of flux distribution inside each circular field of view. First, a horizontal projection of the sky from the zenith down to 55° elevation angle was subdivided into 20×10 squares, and then a 1-s count obtained was given equaly to all of the squares in the field of view of any one counter. At the same moment the similar procedures were applied to the squares within the other two fields of view, respectively. At the next moment the following 1-s counts were added to the squares inside the field of view rotated by $2\pi/45$ around the zenith. After such integration procedure was repeated 45 times, the counting rates accumulated on each squares are divided by the number of summations per square for normalization of detection probability. As a result, a X-ray flux distribution against radial and azimuthal directions, that is, an X-ray image can be composed for every rotation.

Figures 5 and 6 show a time sequence of the X-ray images thus composed for event-1 and event-2, where counts from the three lower energy channels are analyzed. The flux grades shaded are illustrated in six steps from the background to the maximum flux. To estimate a possible time variation of images within one rotation of 45 s, the successive analyses were made using a group of 45-s data shifted by 15-s successively. This interpolation method gives, at a first approximation, time modulations of X-ray images, where 30-s data overlap between one image and the next.

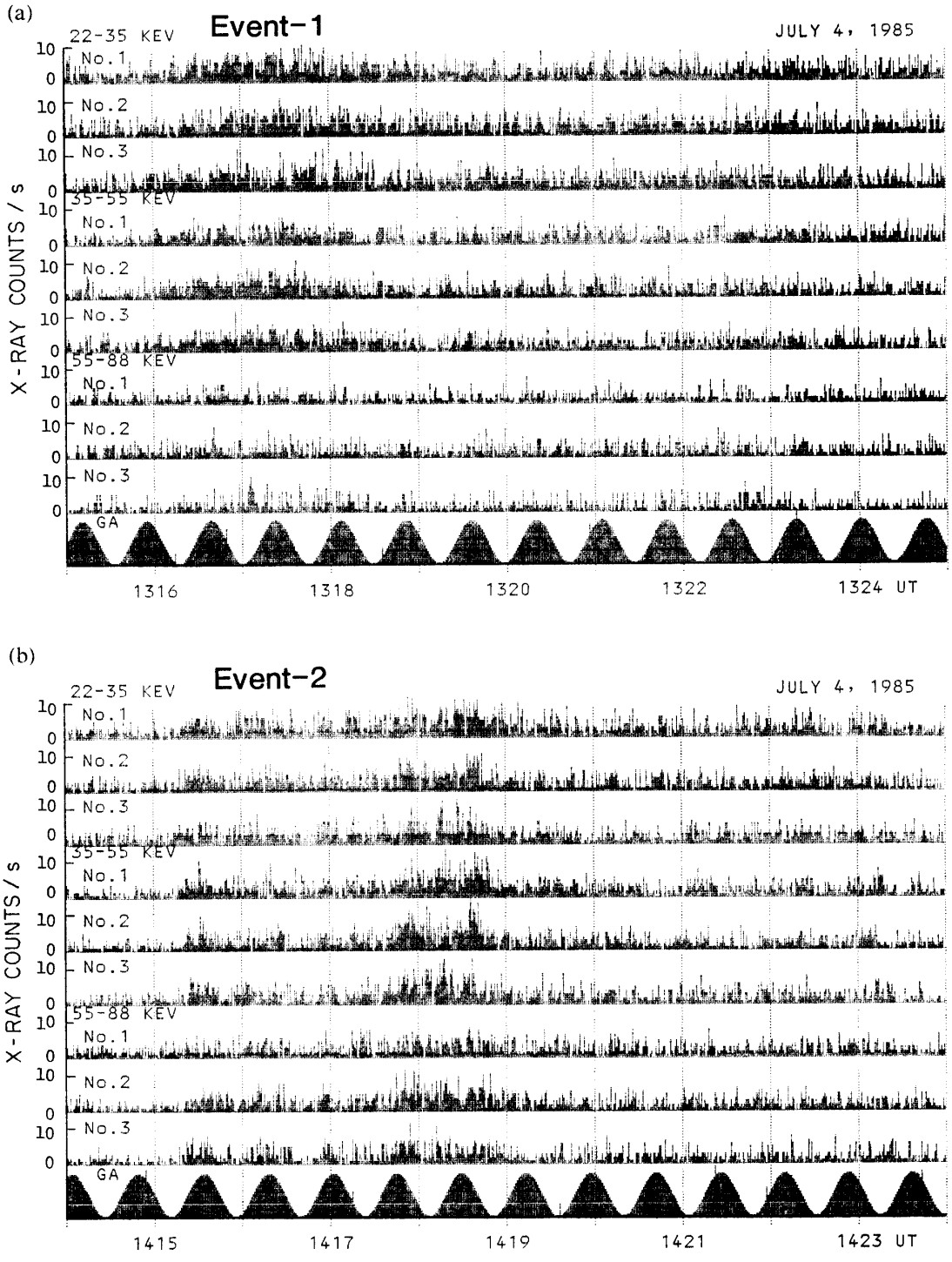

Fig. 4. Time profiles of auroral X-ray fluxes and geomagnetic aspectometer record (GA). 1-s counts from the three different counters are plotted for the three different energy channels. Event-1 on 1315–1325 UT and event-2 on 1414–1424 UT.

In event-1, non-uniformity of flux distribution over the sky is not so distinct, but a little excess of counts is dominant in the geomagnetic northern sector throughout all energy channels. It is obvious from event-2 that the excess flux above the back-

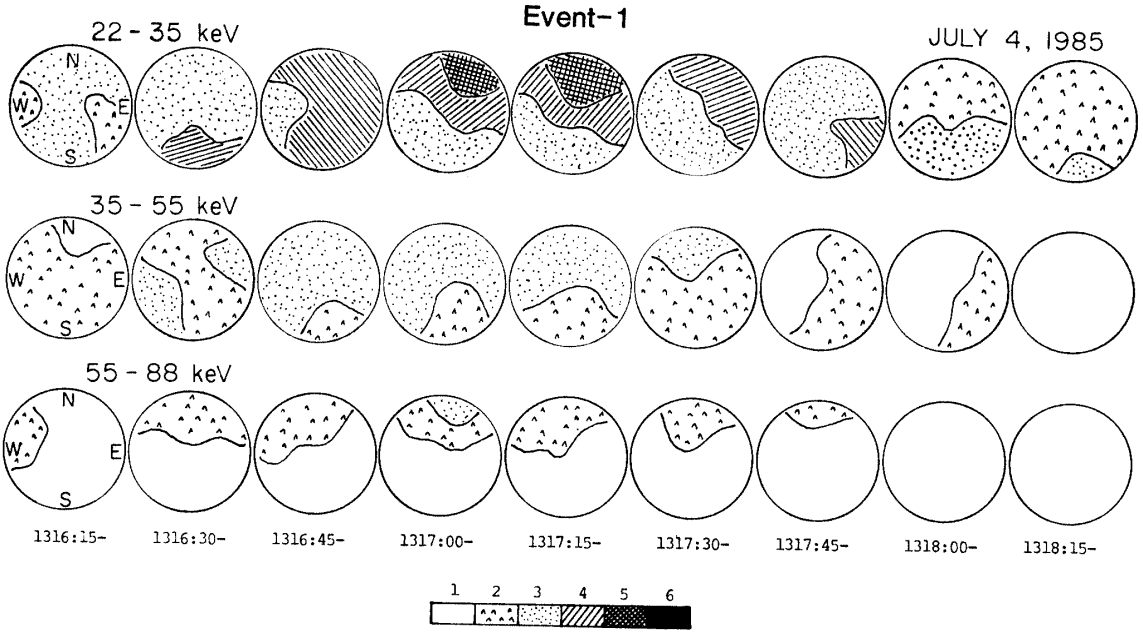

Fig. 5. A time sequence of auroral X-ray images taken every 15 s during the period of 1316:15–1319:00 UT on July 4, 1985. Geomagnetic orientation is indicated in the left side circles.

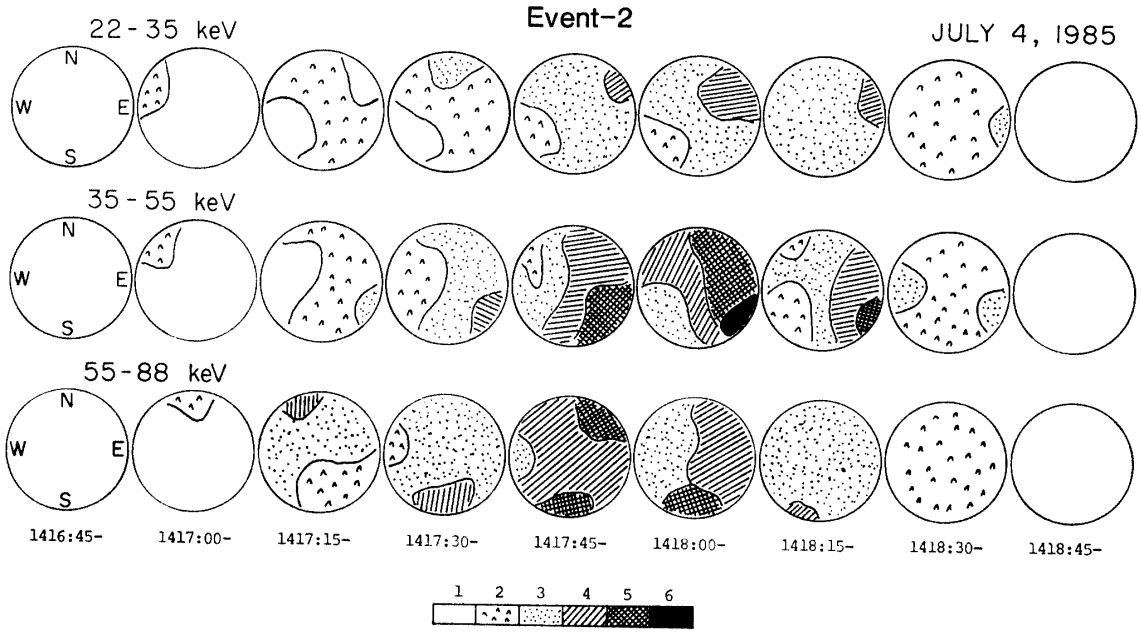

Fig. 6. A time sequence of auroral X-ray images taken every 15 s during the period of 1416:45–1419:30 UT on July 4, 1985. Geomagnetic orientation is indicated in the left side circles.

ground began to appear in the north-east sector. This excess region gradually expanded keeping the anisotropic pattern in the south-east sector and thereafter it faded away step by step. Gross similarity of the anisotropic sector pattern among three different energy channels supports a significance of such composite images.

4. Discussion

X-ray data analyzed in this report were taken in only 24 min, inclusive of two enhancements. Unfortunately, the very low counting rates of the excess fluxes observed made discrimination from statistical fluctuations difficult. The integration method adopted here for image formings introduces a certain degree of ambiguity in spatial pattern, depending on the magnitude of the excess count, even if there exists only one point source of X-rays over the all sky. According to simulated calculations on the assumption of different types of source functions, the estimated region of anisotropic flux distribution reflects approximately the source size when the excess count is as small as three times the background or less.

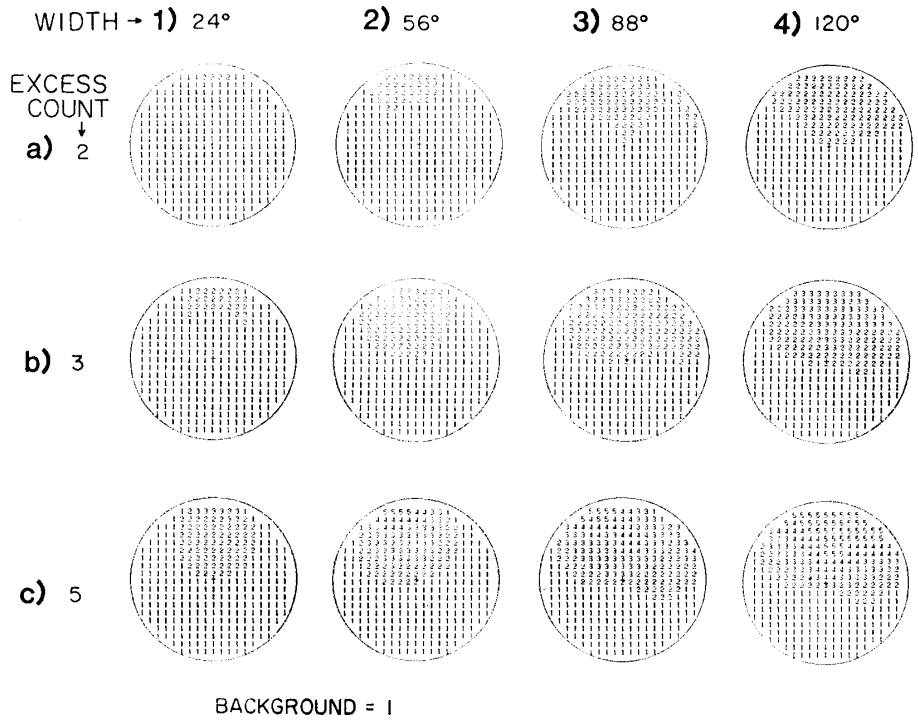

Fig. 7. Results of simulated X-ray images. The source intensities are given by 2, 3 and 5 relative to the background of 1, respectively. The source sizes are taken as 24°, 56°, 88° and 120° in azimuthal width.

Figure 7 shows some examples of the count distributions computed, where the enhanced counts of 2, 3 and 5 in relative to the background count of 1 are given for four different source sizes from 24° to 120°, respectively. The source size is denoted by the azimuthal angle width, within which the excess count selected above was given equally to each counter for every one second. It is obvious from the figure that an apparent size of the excess count region is nearly comparable with the source size when the enhanced count is 2 or 3. On the other hand, the enhanced count of 5 reveals that the computed size of the excess region is not only beyond the source size but also non-uniformity of distribution along the radial direction is amplified with increasing source size. Therefore, it seems that this method of analysis is valid only

for the present small events associated with the maximum enhancement of less than three times the background.

Another ambiguity is caused by atmospheric scatterings of photons during their penetration from the top of atmosphere to a balloon altitude. According to the Monte Carlo simulation given by KODAMA and OGURA (1985), it is estimated that the out-of-focus of auroral X-ray images taken at a depth of 10 g/cm^2 amounts to about 8 km for the present experiment. Taking into account these ambiguities introduced in this experiment, no further information can be derived of fine structures of the pattern composed.

As mentioned earlier, one of the aims of the present balloon campaign was to study the geomagnetic conjugacy. The flight in July is during the austral winter at Syowa Station, when the all-sky camera observation is in operation. But unfortunately it was cloudy at Syowa Station during the flight interval of AZCO-C1, so that no record of visual aurorae were available for direct comparison with the X-ray images shown in the present report. Further comparative studies with other ground-based observations will be done in the near future, particularly in connection with pulsative fluctuations.

Acknowledgments

This work was supported by the National Institute of Polar Research and the Royal Norwegian Council for Scientific and Industrial Research. The authors express their heartfelt thanks to Prof. S. ULLALAND for his valuable comments and advice. Thanks are also due to Mr. A. YONEDA for his assistance on the data processing. The project in Norway and Iceland was supported by Grant-in-Aid for Overseas Scientific Survey 60041085, Ministry of Education, Science and Culture, Japan.

References

CALVERT, W., VOSS, H. D. and SANDERS, T. C. (1985): A satellite imager for atmospheric X-rays. IEEE Trans. Nucl. Sci., **NS-32**, 112–118.

GOLDBERG, R. A., BARCUS, J. R. and TREINISH, L. A. (1982): Mapping of auroral X-rays from rocket overflights. J. Geophys. Res., **87**, 2509–2524.

HIRASIMA, Y., MURAKAMI, H., OKUDAIRA, K., FUJII, M., NISHIMURA, J., YAMAGAMI, T. and KODAMA, M. (1983): Image-forming detectors to observe fine spatial distributions of auroral rays. Mem. Natl Inst. Polar Res., Spec. Issue, **26**, 169–179.

HIRASIMA, Y., MURAKAMI, H., NAKAMOTO, A., OKUDAIRA, K., SUZUKI, H., YAMAGAMI, T., OHTA, S., NAMIKI, M., NISHIMURA, J., MIYAOKA, H., SATO, S., FUJII, R. and KODAMA, M. (1987): A balloon observation of auroral X-ray images in the northern auroral zone. Mem. Natl Inst. Polar Res., Spec. Issue, **47**, 44–55.

IMHOF, W. L., VOSS, H. D., DATLOWE, D. W. and MOBILIA, J. (1985): Bremsstrahlung X-ray images of isolated electron patches at high latitudes. J. Geophys. Res., **90**, 6515–6524.

KODAMA, M. and OGURA, K. (1985): Monte Carlo simulation of auroral X-ray diffusion through the atmosphere. Bull. Yamanashi Med. Coll., **2**, 57–67.

KREMSER, G., BJORDAL, J., BLOCK, L. P., BRONSTAD, K., HAVAG, M., IVERSEN, I. B., KANGAS, J., KORTH, A., MADSEN, M. M., NISKANEN, J., RIEDLER, W., STADSNES, J., TANSKANEN, P., TORKAR, K. M. and ULLALAND, S. L. (1982): Coordinated balloon-satellite observations of energetic particles at the onset of a magnetospheric substorm. J. Geophys. Res., **87**, 4445–

4453.
MAUK, B. H., CHIN, J. and PARKS, G. (1981): Auroal X-ray images. J. Geophys. Res., **86**, 6827–6835.
PARKS, G. K. (1967): Spatial characteristics of auroral-zone X-ray microbursts. J. Geophys. Res., **72**, 215–226.
YAMAGAMI, T., FUJII, M., NISHIMURA, J., MURAKAMI, H., HIRASIMA, Y., KAJIWARA, M., OKUDAIRA, K. and KODAMA, M. (1978): Balloon observations of auroral X-rays in Canada 1. Determination of auroral X-ray illumination regions. J. Geomagn. Geoelectr., **30**, 663–682.

(Received July 9, 1987; Revised manuscript received August 15, 1987)